Stability of Two-Inertia System Using Non-Linear Controller: Application to Drive-Control System of Electric Vehicle

M. Mubin*, S. Ouchi, N. Kodani**, N. Mokhtar*, N. Soin***
*Department of Electrical Engineering, University of Malaya, 50603 Kuala Lumpur, Malaysia.
**Department of Applied Computer Engineering, Tokai University, 1117 Kitakaname, Hiratsuka-shi, Kanagawa, Japan.
E-mail: marizan@um.edu.my

ABSTRACT

The drive-control system of a vehicle is considered as two-inertia system that is the wheel system and the car-body system. This paper firstly presents the stabilization of two-inertia system using a non-linear controller and a disturbance observer. This control system is then applied to a drive-control system of a vehicle with a disturbance observer for estimating the car-body speed. A Lyapunov stability theorem is followed to confirm the stability of the system. The effectiveness of this control system is proved by a satisfactory experimental results.

Keywords: traction control, automatic braking system, disturbance observer, Lyapunov function

1. Introduction

An automobile loses its running stability when it slips due to rapid acceleration, deceleration or braking. The driving force of the automobile is transmitted by a frictional force between the tires and the road surface. This frictional force is a function of the car-body's weight and the tire-road surface's friction coefficient. Furthermore, the friction coefficient is a function of the following parameters: slip ratio determined by a car-body speed, a wheel speed and the condition of the road surface. Due to variations in this friction coefficient, the controlled object treated in this paper is non-linear and subject to disturbances and uncertainties.

Generally, the car-body speed is indispensable information for traction control and anti-lock braking system (ABS). However, it is difficult to measure the absolute car-body speed directly. Thus, the disturbance observer is used to estimate it. The observer to estimate the unknown state variable has been widely used and discussed in [1-4].

Our objective is to develop a control system design to enhance the stability of the automobiles, especially during acceleration, deceleration or braking [3-5]. As to date, many researches have been done on this matter. However, the traction control problems are still far from reaching the final solution and a lot of works such as the robust stability for parameter changes must be done.

2. Control System Design of Two-Inertia System

A two-inertia system as shown in Fig. 1 is considered as a controlled object. This system is expressed by the following equation.

$$\begin{cases} \dot{x}_1 = A_1 x_1 + B_{12} u + B_{11} w, \quad y_1 = C_1 x_1 \\ \dot{x}_2 = A_2 x_2 + B_2 w, \quad w = f(x_1, x_2) \end{cases} \tag{1}$$

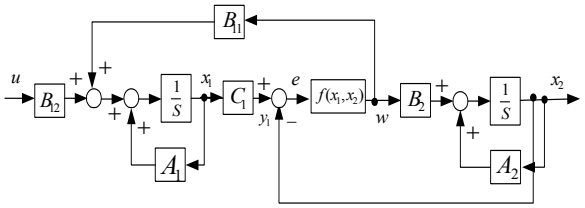

Fig. 1 Block diagram of the controlled object

2.1 Stabilization for Two-Inertia System

In order to stabilize the controlled object above, the performance index is considered as follows:

$$S_1 := \hat{x}_2 - y_1, \quad S_2 := x_{2e} \quad (x_{2e} := \hat{x}_2 - x_2), \tag{2}$$

where $\hat{x}_2$ is assumed to be the estimated value of x_2.
From Eq. (1), the following equation is assumed:

$$\dot{\hat{x}}_2 = A_2 \hat{x}_2 + B_2 \hat{w}. \tag{3}$$

Next, a Lyapunov function is considered as

$$V_{12} = V_1 + V_2, \tag{4}$$

where $V_1 := S_1^T S_1 \ (S_1 \neq 0), \quad V_2 := S_2^T P S_2 \ (S_2 \neq 0, P > 0)$.
Putting

$$u = -(C_1 B_{12})^{-1} (C_1 A_1 x_1 - A_2 \hat{x}_2 - k_1 \frac{S_1}{\|S_1\|} - k_2 S_1)$$

where $|C_1 B_{12}| \neq 0$ and k_1, k_2 are constant values, $\dot{V}_1$ and $\dot{V}_2$ can be obtained as

$$\begin{aligned} \dot{V}_1 &< 2(\gamma \|B_m\| - k_1)\|S_1\| \\ &\quad + \{\lambda_{\max}(B_2 R_1 B_2^T) - 2k_2\}\|S_1\|^2 + w_e^T R_1^{-1} w_e \end{aligned}, \tag{5}$$

$$\dot{V}_2 \leq -x_{2e}^T Q x_{2e} + w_e^T R_2^{-1} w_e \leq w_e^T R_2^{-1} w_e \tag{6}$$

where $B_m := B_2 - C_1 B_{11}$, $w_e := \hat{w} - w$, $\gamma > \|w\|$, $R_1 > 0$, $R_2 > 0$ (R_1, R_2: free parameter).
Then, from Eq. (5) and (6), the following equation can be obtained:

$$\begin{aligned} \dot{V}_{12} &= \dot{V}_1 + \dot{V}_2 \\ &< 2(\gamma \|B_m\| - k_1)\|S_1\| + \{\lambda_{\max}(B_2 R_1 B_2^T) - 2k_2\}\|S_1\|^2 \\ &\quad + w_e^T (R_1^{-1} + R_2^{-1}) w_e. \end{aligned} \tag{7}$$

When $k_1 \geq \gamma \|B_m\|$ and $k_2 \geq \frac{1}{2}\lambda_{\max}(B_2 R_1 B_2^T)$,

$$\dot{V}_{12} < w_e^T (R_1^{-1} + R_2^{-1}) w_e$$

is obtained. However, $\dot{V}_{12} < 0$ cannot be obtained

because $R_1, R_2 > 0$. So, the next disturbance observer is considered as an estimation system.

2.2 Disturbance Observer

A disturbance observer such as $\hat{w} \to w\,(t \to \infty)$ is designed. From Eq. (1), the controlled object for the disturbance observer design is considered as follows:

$$\dot{x}_1 = A_1 x_1 + B_{12} u + B_{11} w. \tag{8}$$

Next, the following equation is assumed:

$$\dot{\hat{x}}_1 = A_1 \hat{x}_1 + B_{12} u + B_{11} u_o + B_{11} \hat{w}. \tag{9}$$

By subtracting Eq. (8) from (9), Eq. (10) can be obtained.

$$\dot{x}_{1e} = A_1 x_{1e} + B_{11} u_o + B_{11} w_e, \tag{10}$$

where $x_{1e} := \hat{x}_1 - x_1, \quad w_e := \hat{w} - w$.

In order to obtain $w_e \to 0$, the following Lyapunov function is considered:

$$V_3 = w_e^T w_e. \tag{11}$$

Here, $\dot{w} \approx 0$ is assumed if $\mathrm{Re}\,\lambda(\hat{w}) >> \mathrm{Re}\,\lambda(w)$. Furthermore, put

$$\hat{w} := L x_{1e} \quad (L := k_3 (GB_{11})^T G), \tag{12}$$

$\dot{V}_3$ can be expressed as

$$\dot{V}_3 = 2k_3 \cdot w_e{}^T (GB_{11})^T (GB_{11}) w_e. \tag{13}$$

When $k_3 < 0$, $\dot{V}_3 < 0$ $(w_e \neq 0)$ can be obtained because $|GB_{11}| \neq 0$. Then, $\hat{w} \to w\,(t \to \infty)$ is obtained.

The block diagram for the disturbance observer is shown in Fig. 2.

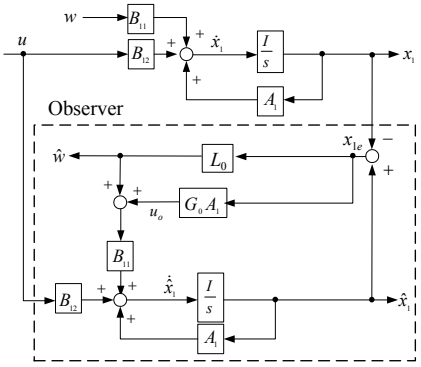

Fig. 2 Disturbance observer

2.3 Combined System

The combined system consists of the controlled object and the disturbance observer is then considered. From Eq. (7) and (13),

$$\begin{aligned}\dot{V} &= \dot{V}_1 + \dot{V}_2 + \dot{V}_3 \\ &< 2(\gamma \|B_m\| - k_1)\|S_1\| + \left\{\lambda_{\max}\left(B_2 R_1 B_2^T\right) - 2k_2\right\}\|S_1\|^2 \\ &\quad + \left\{\lambda_{\max}\left(R_1^{-1} + R_2^{-1}\right) + 2k_3 \lambda_{\max}\left(GB_{11}\right)^T \left(GB_{11}\right)\right\}\|w_e\|^2\end{aligned}$$

When

$$A_2^T P + P A_2 + P B_2 R_2 B_2^T P + Q = 0 \quad (Q \geq 0, P > 0),$$

$$k_1 \geq \gamma \|B_m\| > 0 \quad (B_m := B_2 - C_1 B_{11}),$$

$$k_2 \geq \frac{1}{2}\lambda_{\max}\left(B_2 R_1 B_2^T\right) > 0, \quad R_1 > 0,$$

$$k_3 \leq -\frac{\lambda_{\max}(R_1^{-1} + R_2^{-1})}{2\lambda_{\max}(GB_{11})^T (GB_{11})} < 0, \quad \|w\| < \gamma,$$

$\dot{V} < 0$ can be obtained. By following the Lyapunov stability theorem, the control purpose $x_2 \to y_1\,(t \to \infty)$ is obtained. Therefore, the control law to stabilize the controlled object can be obtained as follows:

$$u = R\left(F_1 \hat{x}_2 + F_2 x_1 - k_1 \frac{S_1}{\|S_1\|} - k_2 S_1\right)$$

where

$S_1 := \hat{x}_2 - C_1 x_1, R := -(C_1 B_{12})^{-1}, F_1 := -A_2, F_2 := C_1 A_1$

The block diagram of the combined system is shown in Fig. 3.

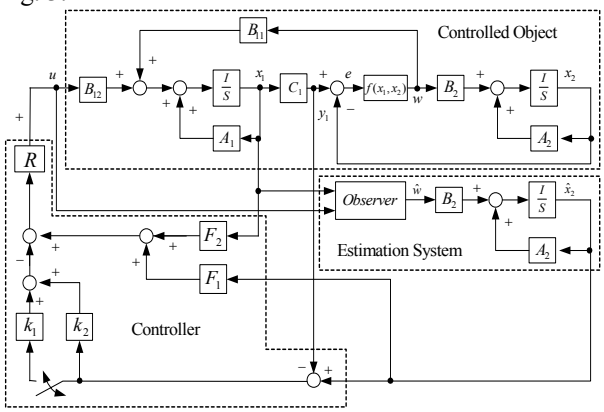

Fig. 3 Combined Systems

3. Application to Driving System

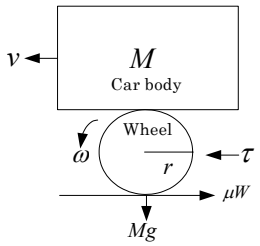

Fig. 4 Vehicle Model

The obtained results from the previous section are applied into the driving system of the automobiles. The driving system is considered as depicted in Fig. 4. The equations of motion of the system can be expressed as follows:

$$\begin{cases}\dot{\omega} = a_2\omega + b_{m2}\mu + b_2\tau, \quad \dot{v} = a_1 v + b_{m1}\mu \\ \dot{\tau} = a_t\tau + b_t\tau_i\,,\ \mu = f(\lambda)\end{cases}, \tag{14}$$

where

$$\begin{bmatrix} a_2 := -B/J, b_{m2} := -Wr/J, b_2 := 1/J \\ a_1 := -C/M, b_{m1} := W/(Mr), b_t := 1/T_f \\ a_t := -1/T_f\,, \lambda := (\omega - v)/\max(\omega, v) \end{bmatrix}$$

All parameters used in Eq. (14) are defined in Table 1. The block diagram shown in Fig. 5 can be constructed by using Eq. (14).

Table 1 Wheel and vehicle parameters

τ	Tractive torque	ω	Angular speed of the wheel
M	Vehicle mass	g	Acceleration of gravity
C	Friction of vehicle	v	Car-body speed
W	Vehicle weight	u	Torque input
J	Moment of inertia of the wheel	T_f	Torque system parameter
r	Wheel radius		

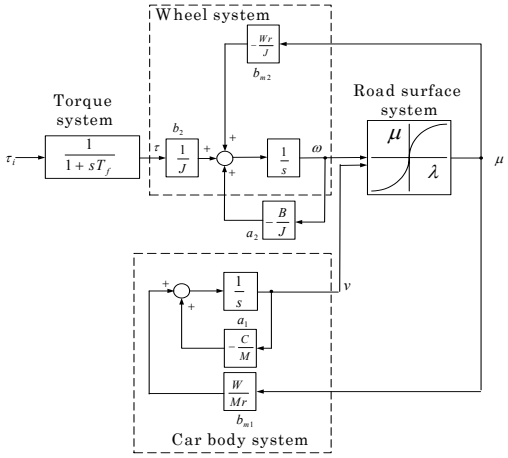

Fig. 5 Block diagram of the vehicle system

From Eq. (14), the equation of motion of the driving system can be expressed as follows

$$\begin{cases} \dot{\omega} = a_2\omega + b_2\tau + b_{m2}\mu \\ y_1 = a\omega, \quad \dot{v} = a_1 v + b_{m1}\mu \\ \mu = f(\lambda) \quad [\lambda := (\omega - v)/\max(\omega, v)]. \end{cases}$$

Since μ can not be measured, the disturbance observer is used to estimate μ and the estimation value of the car body speed $\hat{v}$ is calculated from $\hat{\mu}$. Using Eq. (12), the following equation can be expressed:

$$\hat{\mu} = L\omega_e \ (L = k_3 \cdot b_{m2}).$$

From the discussion above, the control law can be obtained as follows:

$$\tau = R\left(F_1\hat{v} + F_2\omega - k_1\frac{S_1}{|S_1|} - k_2 S_1 \right) + \tau_r$$

where τ_r is a torque reference value, and

$$R := -1/(ab_2), \quad F_1 := -a_1, \quad F_2 := aa_2,$$
$$R_1 > 0, \ R_2 = -(2a_1P + Q)/b_{m1}^2 P^2 > 0 \ \ (P > 0, \ Q \geq 0),$$
$$k_1 \geq \gamma |b_{m1} - ab_{m2}|, \quad k_2 \geq b_{m1}^2 R_1/2,$$
$$k_3 \leq -(1/R_1 + 1/R_2)/2b_{m2}^2, \quad |\mu| < \gamma.$$

The block diagram of the control system can be drawn as in Fig. 6.

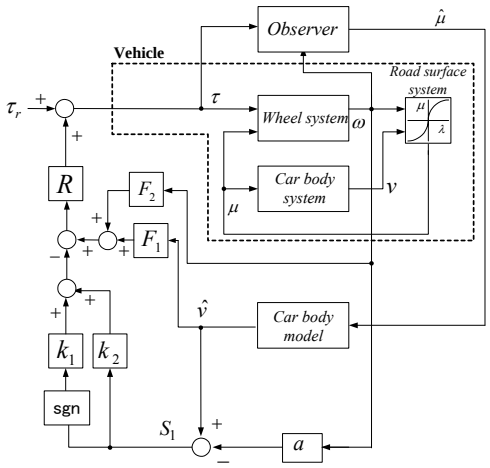

Fig. 6 Control System Design

Refer to Fig. 6, the structure of the control system can be divided into two conditions that is $S \neq 0$ and $S \approx 0$. $S \neq 0$ is the condition in which slip does not occur, the time variation for the estimated value of car-body speed $\hat{v}$ and the vehicle speed ω are small. Therefore, it can be considered that $\dot{\hat{v}}, \dot{\omega} \to 0$. This system is known as τ control system. On the other hand, for the condition of $S \approx 0$, $\lambda = \lambda_0$ is obtained at $\omega \geq v$, where λ_0 is the reference value of slip ratio. Meanwhile, at $\omega < v$, $\lambda = -\lambda_0$ is obtained where full control can be done. This control system is called λ control system.

4. Experimental Results

In order to check the feasibility of the designed controller, it is implemented into a specially modified experimental device as shown in Fig. 7. The device consists of two rotating wheels, which represent the vehicle wheel and the car-body respectively as labeled.

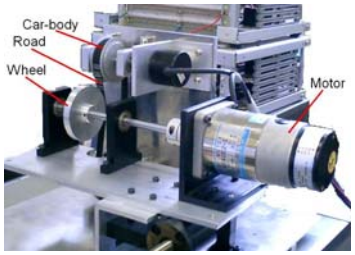

Fig. 7 Experimental Device

Parameters of the experimental device are shown in Table 5 while Table 6 shows the controller gains that have been used in this control system. A different value of gains are used for different road conditions with slip and without slip.

The experimental results for the wheel accelerating on the slippery road under non-control are shown in Fig. 8. From Fig. 8(a) and (b), it is shown that when an

approximately 0.01 Nm torque is given, the wheel starts rotating. However, the car-body is not moving and this indicates that the large slip occurs.

Meanwhile, from Fig. 8(c) and (d), it can be observed that after the wheel starts accelerating, the slip ratio goes up to $\lambda = 1$ for 6 seconds before it decreases to about $\lambda = 0.2$. However, as the speed of the wheel increases, the slip ratio seems to be increased.

Table 2 Experimental device parameters

P	Motor power [W]	20
M	Vehicle mass [kg]	0.06
C	Friction of the vehicle [Nms]	0.001
B	Friction of the wheel [Nms]	$2.5\text{x}10^{-5}$
W	Vehicle weight [N]	0.588
J	Moment of inertia for the wheel [kgm^2]	$4.0\text{x}10^{-5}$
r	Wheel radius [m]	0.03
T_f	Time constant of the torque system [sec]	0.1
τ_i	Torque reference (with slip) [Nm]	0.009
τ_i	Torque reference (without slip) [Nm]	0.005

Table 3 Controller gains of the experimental device

	With slip	Without slip
R_1	$3.75\text{x}10^{-3}$	$3.75\text{x}10^{-3}$
R_2	$2.66\text{x}10^{-5}$	$2.66\text{x}10^{-5}$
F_1R	$-8.33\text{x}10^{-7}$	$-8.33\text{x}10^{-7}$
F_2R	$2.5\text{x}10^{-5}$	$2.5\text{x}10^{-5}$
k_1R	$-6.8\text{x}10^{-3}$	$-6.8\text{x}10^{-3}$
k_2R	-0.01	-10^{-5}
k_3	$-9.75\text{x}10^{-2}$	$-9.75\text{x}10^{-2}$
L	43	43
λ_0	0.2	0.2
γ	0.2	0.2

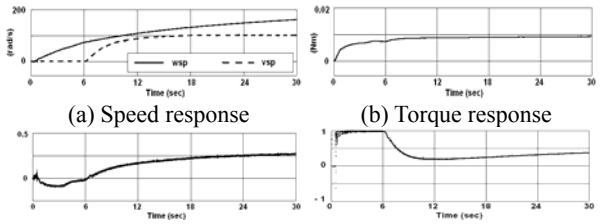

(a) Speed response (b) Torque response

(c) Friction coefficient, μ (d) Slip ratio, λ

Fig. 8 Experimental results for non-control case

Two separated experiments have been carried out since it is difficult to run the experiment for both conditions of normal road and slippery road at the same time. The experimental results for the control case under the normal road condition are shown in Fig. 9(i), while the experimental results under the slippery road condition are given in Fig. 9(ii). From Fig. 9, it is shown that the wheel speed can be controlled at the slip ratio of approximately $\lambda = 0.2$ when an input torque of about 0.01 Nm is given.

Meanwhile, from Fig. 9(e), it can be seen that switching does not occur when the wheel accelerating on the normal road. In this case, τ control system is taking place. However, switching occurs in Fig. 9(ii-e) shows that the λ control system is operating when the wheel is accelerating on the slippery road.

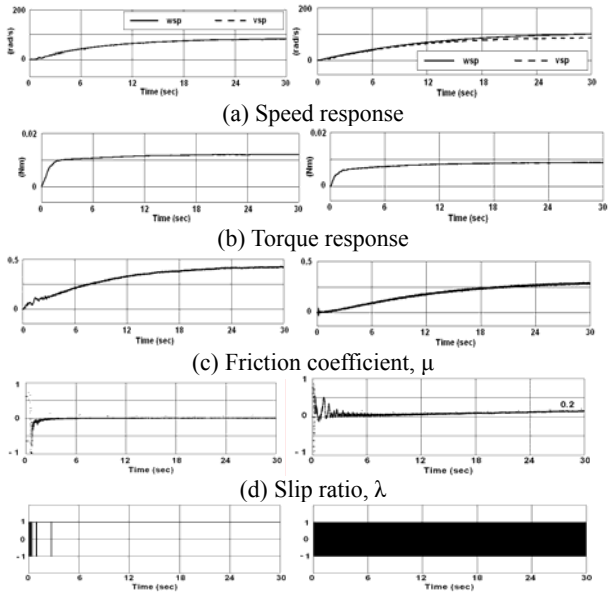

(a) Speed response

(b) Torque response

(c) Friction coefficient, μ

(d) Slip ratio, λ

(e) Switching function

(i) Normal road (ii) Slippery road

Fig. 9 Experimental results for control case

5. Conclusion

From the experimental results, it has been proved that by using the proposed control system, an appropriate torque can be generated even though the road condition changes from the normal road to the slippery road or vice versa.

6. References

[1] S. Ouchi, K. Yano, "Control of Oscillating Multi-mass system with Gear Backlash by Digital Observer", T. IEE Japan, Vol. 110-D, No. 4, pp. 410-417 (1990) – In Japanese.

[2] J.O'Reilly, "Minimal Order Observer for Linear Multivariable Systems Disturbances", Int. J. Control, 28, pp. 743-751 (1978)

[3] M. Mubin, K. Moroda, S. Ouchi, and M Anabuki : "Model Following Sliding Mode Control of Automobiles Using a Disturbance Observer", Proceeding of SICE Annual Conference, pp. 1384-1389 (2003)

[4] C. Unsal, and P. Kachroo, "Sliding Mode Measurement Feedback Control for Antilock Braking Systems", IEEE Trans. Of Control System Tech. Vol. 7, No. 2, pp. 271-281 (1999)

[5] H. Sado, S. Sakai and Y. Hori, "Road Condition Estimation for Traction Control in Electric Vehicle", IEEE International Symposium on Industrial Electronics, pp. 973-978 (1999).